

Syntheses and crystal structures of Ge-bearing layered carbides $Zr_2Al_4C_5$ and $Zr_3Al_4C_6$

Keita SUGIURA, Tomoyuki IWATA, Naohiro SUNADA, Shinobu HASHIMOTO, Hiromi NAKANO*
and Koichiro FUKUDA†

Department of Environmental and Materials Engineering, Nagoya Institute of Technology, Nagoya 466-8555

*Electron Microscope Laboratory, Ryukoku University, Otsu 520-2194

Two types of new quaternary carbide solid solutions, $(ZrC)_2Al_3[Al_{1-x}Ge_x]C_3$ ($x = 0.07$) and $(ZrC)_3Al_3[Al_{1-y}Ge_y]C_3$ ($y = 0.04$), have been synthesized and characterized using a laboratory X-ray powder diffractometer (XRPD) and a transmission electron microscope (TEM) equipped with an energy dispersive X-ray analyzer (EDX). With the former carbide, the layered structure was imaged by TEM and the solubility of Ge in the crystal was confirmed by EDX. The crystal structures of both carbides were refined by the Rietveld analysis of the XRPD data. These carbides have been found to form a homologous series with the general formula $(ZrC)_mAl_3[Al_{1-z}Ge_z]C_3$ ($0 \leq z \leq 0.07$), where $m = 2$ and 3 . The crystal structures can be regarded as intergrowth structures, consisting of the NaCl-type $[Zr_mC_{m+1}]$ slabs separated by the Al_4C_3 -type $[Al_{4-z}Ge_zC_4]$ layers.

©2009 The Ceramic Society of Japan. All rights reserved.

Key-words : Layered carbides, Solid solutions, Crystal structures, Powder diffraction, Rietveld refinement

[Received July 22, 2008; Accepted October 16, 2008]

1. Introduction

In the system Zr-Al-C, two types of new ternary carbides, $Zr_2Al_4C_5$ and $Zr_3Al_4C_6$, have been recently established; they were synthesized at 2073 K and structurally characterized by X-ray powder diffraction (XRPD) method.¹⁾ These carbides form a homologous series with the general formula $(ZrC)_mAl_3C_3$ ($m = 2$ and 3). The crystal structures, belonging to the same space group $R\bar{3}m$, can be regarded as intergrowth structures where the Al_4C_3 -type $[Al_4C_4]$ layers are the same, while the NaCl-type $[Zr_mC_{m+1}]$ layers increase in thickness with increasing m value. At lower temperatures than 2073 K (e.g., 1973 K), considerable amounts of Si component have been found to dissolve into the $[Al_4C_4]$ layers of $(ZrC)_mAl_4C_3$ to stabilize the crystal structures.^{2,3)} Thus, the ternary carbides $(ZrC)_mAl_4C_3$ are considered to be the end members of solid solutions $(ZrC)_m(Al, Si)_4C_3$.¹⁾ Because the atomic scattering factors for Al and Si are almost the same, the Si and Al atoms were assumed to be randomly distributed over the same sites in the Al_4C_3 -type layers, although there might be the site preference of these atoms.

The NaCl-type $[Zr_mC_{m+1}]$ slabs and Al_4C_3 -type $[Al_4C_4]$ layers in $(ZrC)_mAl_4C_3$ share the carbon-atom network at their boundaries; the C-C distances are ~ 0.332 nm for both $m = 2$ and $m = 3$.¹⁾ On the other hand, the C-C distance of ZrC crystal is 0.330 nm ($= a(ZrC)/\sqrt{2}$) and that of Al_4C_3 is 0.334 nm ($= a(Al_4C_3)$), where $a(ZrC)$ and $a(Al_4C_3)$ represent the a -axis lengths of the ZrC and Al_4C_3 crystals, respectively. These distances are close to each other, and also to those of the carbon-atom networks in $(ZrC)_mAl_4C_3$. Fukuda et al. have therefore concluded that the closeness of the C-C distances between the ZrC and Al_4C_3 crystals, being expressed by the equation $a(ZrC)/\sqrt{2} \approx a(Al_4C_3)$, is the principal reason for the formation of the layered carbides in the

ternary system.^{1,4)} This principle also holds for other layered carbides $(ZrC)_mAl_3C_2$ ($m = 2$ and 3)^{4,5)} as well as $(ZrC)_m(Al, Si)_4C_3$.

From analogy with the existence of the $(ZrC)_m(Al, Si)_4C_3$ solid solutions, we have expected the formation of new layered carbides in the quaternary system Zr-Al-Ge-C. Because the atomic scattering factors for Al and Ge are quite different, we have succeeded in determining the site preference of Ge atoms in the crystal structures.

2. Experimental procedure

2.1 Syntheses of new carbides

In the reacted ZrC-Al₄C₃-Ge-C mixtures, two types of new quaternary carbides were initially recognized by their very similar diffraction patterns to those of the $(ZrC)_m(Al, Si)_4C_3$ solid solutions.^{2,3)} Since the present specimens are free from Si component, the new carbides are most probably of Ge-dissolved $(ZrC)_mAl_4C_3$ solid solutions. We obtained, by the following procedures, the two types of powder samples; one was consisting mainly of $(ZrC)_2(Al, Ge)_4C_3$ (sample S-A) and the other was mainly composed of $(ZrC)_3(Al, Ge)_4C_3$ (S-B).

The reagent-grade chemicals of ZrC (99.9%, KCL Co., Ltd., Saitama), Al_4C_3 (KCL, 99.9%), Ge (99.99%, Mitsuwa Chemical Co., Ltd., Osaka) and C (KCL, 99.7%) were mixed in two different molar ratios of $[ZrC:Al_4C_3:Ge:C] = [2:4:0.2:0.15]$ for S-A and $[ZrC:Al_4C_3:Ge:C] = [3:1.2:0.24:0.18]$ for S-B. Each of the well-mixed chemicals was pressed into pellets ($\phi 13$ mm \times 10 mm), heated at 1973 K for 2 h in inert gas atmosphere of Ar, followed by cooling to ambient temperature by cutting furnace power. Both reaction products were slightly sintered polycrystalline materials. They were finely ground to obtain powder specimens. Small amounts of ZrC, Ge (metal) and Al_4C_3 crystallites coexisted in both samples, the latter of which were completely removed by dissolution with acid solution.

† Corresponding author: K. Fukuda; E-mail: fukuda.koichiro@nitech.ac.jp

2.2 Characterization

XRPD intensities were collected on a diffractometer (X'Pert PRO Alpha-1, PANalytical B. V., Almelo, the Netherlands) equipped with a high speed detector in Bragg-Brentano geometry using monochromatized Cu K α_1 radiation (45 kV, 40 mA) in a 2θ range from 10.0062° to 148.9019° (an accuracy in 2θ of $\pm 0.0001^\circ$). The automatic divergence slit was employed to maintain an illumination length of 5 mm on the sample. Thus, the quantitative profile intensities were collected over the whole 2θ range. Other experimental conditions were: continuous scan, total of 8792 datapoints and total experimental time of 5.9 h. The crystal-structure models were visualized with the computer program VESTA.⁶⁾

The powder specimen of S-A was examined using a transmission electron microscope (JEM 3000F, JEOL Ltd., Tokyo) operated at 300 kV and equipped with an energy dispersive X-ray analyzer (EDX; VOYAGER III, NORAN Instruments, Middleton, WI, USA). The powder particles were deposited with ethyl alcohol on a copper grid. A selected area electron diffraction (SAED) pattern and corresponding lattice image were obtained. A chemical analysis was made for seven crystal frag-

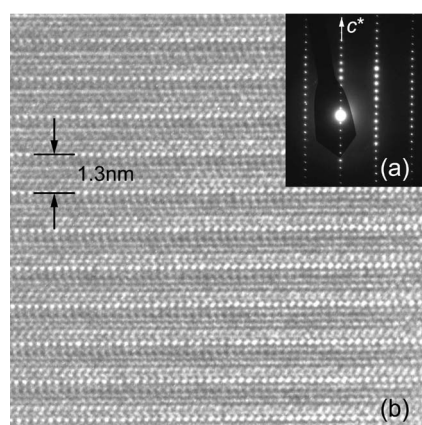


Fig. 1. (a) Selected-area electron diffraction pattern and (b) corresponding lattice fringe image showing periodicity of about 1.3 nm ($= c/3$). Incident beam perpendicular to the c -axis. Sample $(\text{ZrC})_2(\text{Al},\text{Ge})_4\text{C}_3$ in S-A.

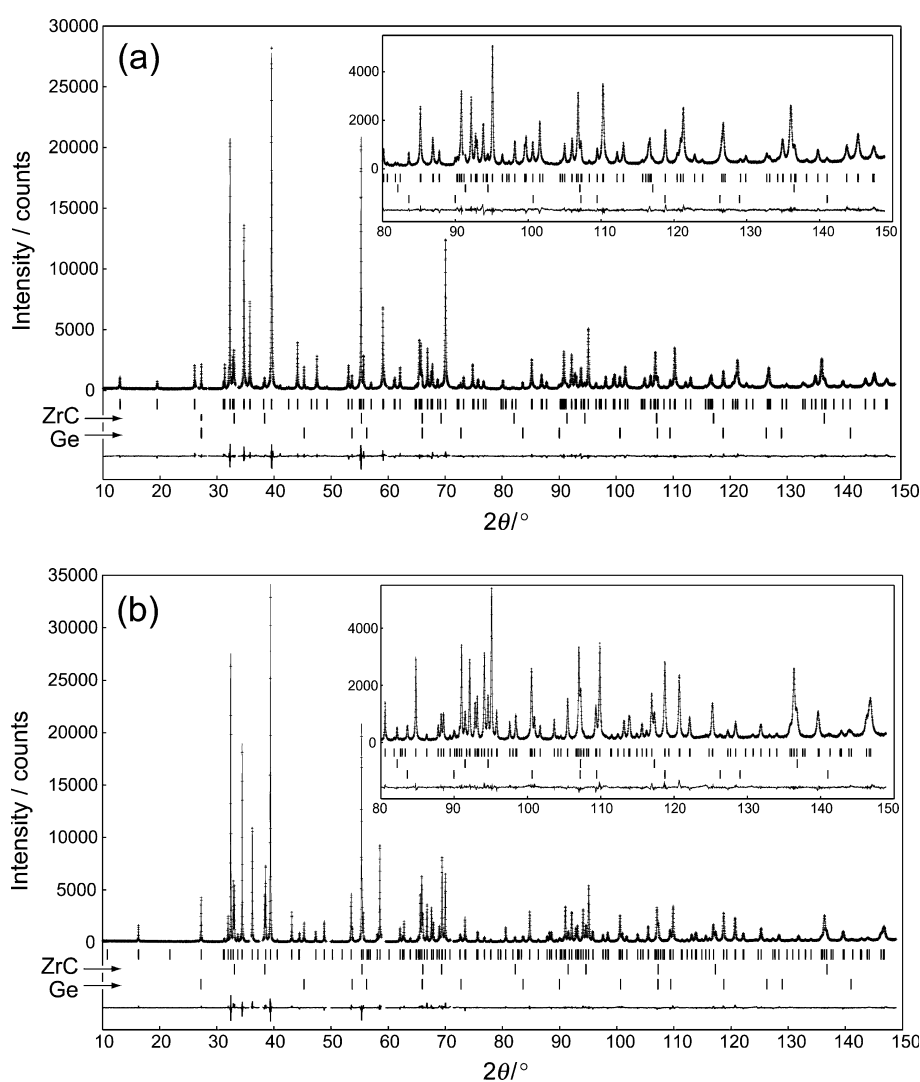


Fig. 2. Comparison of the observed diffraction patterns (symbol: +) with the corresponding calculated patterns (upper solid lines). The difference curves are shown in the lower part of the diagrams. Upper vertical bars in each diagram indicate the positions of possible Bragg reflections. The profile intensities for S-A in (a) and S-B in (b).

ments of $(ZrC)_2(Al,Ge)_4C_3$ to determine the concentration of Ge. The correction was made by the ZAF routines.

3. Results and discussion

3.1 Structure refinement

The SAED pattern (Fig. 1(a)) of $(ZrC)_2(Al,Ge)_4C_3$ in S-A was successfully indexed with a hexagonal unit cell with dimensions of $a \approx 0.33$ nm and $c \approx 4.1$ nm. The corresponding lattice image (Fig. 1(b)) strongly suggests that the crystal structure is built up from stacking combinations of two basic sheets. The presence of Ge atoms within the crystal has been well confirmed by the EDX analysis. The average atom ratios [Zr:Al:Ge] were found to be [64.6(28):35.0(28):0.4(2)], which is equivalent to [Al:Ge] = [3.97(2):0.03(2)] on the basis of Al + Ge = 4. The EDX analysis showed that the atom ratios varied widely from crystal fragment to fragment, resulting in a relatively large standard deviation of the Ge concentration.

Initial structural parameters of $(ZrC)_2(Al,Ge)_4C_3$ in S-A and $(ZrC)_3(Al,Ge)_4C_3$ in S-B were taken from those determined by Sugiura et al. for $(ZrC)_2Al_4C_3$ and $(ZrC)_3Al_4C_3$, respectively.¹⁾ The structural parameters were individually refined by the Rietveld method using the computer program RIETAN-FP.⁷⁾ The structure models of ZrC and Ge (metal) were added into the refinement as additional phases. A Legendre polynomial was fitted to background intensities with twelve adjustable parameters. The split Pearson VII function⁸⁾ was used to fit the peak profile. At the initial stage of the refinement process, the Al and Ge atoms were assumed to be randomly distributed over the four Al sites in the crystal structures without any constraints on occupancies. The site occupancies of Ge in the three Al sites eventually converged to zero or below for both crystal structures, indicating that the Ge atoms were exclusively distributed on one of the other Al sites (denoted by T). Based on the final site occupancies of Ge atoms in the T sites, the chemical formulas were determined to be $(ZrC)_2Al_3[Al_{0.930(8)}Ge_{0.070(8)}]C_3$ in S-A and $(ZrC)_3Al_3[Al_{0.958(11)}Ge_{0.042(11)}]C_3$ in S-B, where the numbers in parentheses indicate standard deviations. The isotropic atomic

displacement parameters (B) of the Al sites (Al1, Al2 and Al3) were constrained to have the same value and those of the C sites as well. The reliability indices⁹⁾ for the final result of S-A were $R_{wp} = 7.32\%$, $S = 1.65$ and $R_p = 5.41\%$ ($R_B = 1.35\%$ and $R_F = 0.89\%$ for $(ZrC)_2Al_3[Al_{0.93}Ge_{0.07}]C_3$) (Fig. 2(a)) and those of S-B were $R_{wp} = 7.48\%$, $S = 1.57$ and $R_p = 5.41\%$ ($R_B = 1.65\%$ and $R_F = 0.99\%$ for $(ZrC)_3Al_3[Al_{0.96}Ge_{0.04}]C_3$) (Fig. 2(b)). Crystal data are given in Tables 1 and 2, and the final atomic positional and B parameters are given in Tables 3 and 4.

The atom ratios [Al:Ge] that were determined by XRPD for the layered carbides in S-A (= [3.93:0.07]) and S-B (= [3.96:0.04]) are of the average values for those of the individual powder particles. The EDX analysis of the former carbide showed that each crystal fragment was rather heterogeneous in chemical composition, with the atom ratios [Al:Ge] almost rang-

Table 3. Structural Parameters for $(ZrC)_2Al_3[Al_{0.93}Ge_{0.07}]C_3$

Site	Wyckoff position	x	y	z	$100 \times B/\text{nm}^2$
Zr1	3a	0	0	0.6341(2)	0.55(4)
Zr2	3a	0	0	0.9028(2)	0.52(4)
Al1	3a	0	0	0.0747(2)	1.14(4)
Al2	3a	0	0	0.3560(2)	1.14
Al3	3a	0	0	0.4550(2)	1.14
T^{*1}	3a	0	0	0.1800(2)	0.76(7)
C1 ^{*2}	3a	0	0	0	0.50(6)
C2	3a	0	0	0.1321(4)	0.50
C3	3a	0	0	0.2687(7)	0.50
C4	3a	0	0	0.4036(5)	0.50
C5	3a	0	0	0.5316(2)	0.50

^{*1}Site occupancy: 0.930(8) Al and 0.070(8) Ge.

^{*2} z of C1 atom is fixed.

Table 1. Crystal Data for $(ZrC)_2Al_3[Al_{0.93}Ge_{0.07}]C_3$

Chemical composition	$Zr_2Al_{3.93}Ge_{0.07}C_5$
Space group	$R\bar{3}m$
a/nm	0.332256 (2)
c/nm	4.09434 (2)
V/nm^3	0.391436 (3)
Z	3
D_s/Mgm^{-3}	4.50

Table 2. Crystal Data for $(ZrC)_3Al_3[Al_{0.96}Ge_{0.04}]C_3$

Chemical composition	$Zr_3Al_{3.96}Ge_{0.04}C_6$
Space group	$R\bar{3}m$
a/nm	0.331897 (2)
c/nm	4.89854 (3)
V/nm^3	0.467309 (5)
Z	3
D_s/Mgm^{-3}	4.86

Table 4. Structural Parameters for $(ZrC)_3Al_3[Al_{0.96}Ge_{0.04}]C_3$

Site	Wyckoff position	x	y	z	$100 \times B/\text{nm}^2$
Zr1	3a	0	0	0.3048(7)	0.52(7)
Zr2	3a	0	0	0.6927(7)	0.61(8)
Zr3	3a	0	0	0.9174(7)	0.64(8)
Al1	3a	0	0	0.0732(8)	1.37(9)
Al2	3a	0	0	0.1545(7)	1.37
Al3	3a	0	0	0.4483(7)	1.37
T^{*1}	3a	0	0	0.5369(7)	1.07(11)
C1 ^{*2}	3a	0	0	0	0.59(8)
C2	3a	0	0	0.1118(8)	0.59
C3	3a	0	0	0.2203(6)	0.59
C4	3a	0	0	0.3887(6)	0.59
C5	3a	0	0	0.4982(9)	0.59
C6	3a	0	0	0.6106(3)	0.59

^{*1}Site occupancy: 0.958(11) Al and 0.042(11) Ge.

^{*2} z of C1 atom is fixed.

ing from [3.99:0.01] to [3.95:0.05]. Thus, the chemical variation was feasibly within the solid-solution range of $0 \leq x \leq 0.07$ for $(\text{ZrC})_2\text{Al}_3[\text{Al}_{1-x}\text{Ge}_x]\text{C}_3$. In a similar manner as above, the latter carbide solid solution would be satisfactorily represented by the general formula of $(\text{ZrC})_3\text{Al}_3[\text{Al}_{1-y}\text{Ge}_y]\text{C}_3$ with $0 \leq y \leq 0.04$.

Quantitative X-ray analysis with correction for microabsorption according to Brindley's procedure¹⁰⁾ was implemented in the program RIETAN-FP. The phase composition of S-A, excluding Al_4C_3 , was determined to be 96.5 mass% $(\text{ZrC})_2\text{Al}_3[\text{Al}_{0.93}\text{Ge}_{0.07}]\text{C}_3$, 1.6 mass% ZrC and 1.9 mass% Ge. The bulk chemical composition in molar ratios was found from

calculation to be $[\text{Zr}:\text{Al}:\text{Ge}:\text{C}] = [2:3.82:0.16:4.92]$, the $[\text{Zr}:\text{Ge}]$ ratios of which is almost equivalent to that of the starting mixture ($[\text{Zr}:\text{Ge}] = [2:0.2]$). In a similar manner as above, the phase composition of S-B was determined to be 89.4 mass% $(\text{ZrC})_3\text{Al}_3[\text{Al}_{0.96}\text{Ge}_{0.04}]\text{C}_3$, 8.0 mass% ZrC and 2.6 mass% Ge, which corresponds to the molar ratios $[\text{Zr}:\text{Al}:\text{Ge}:\text{C}] = [3:3.50:0.19:5.65]$. Thus, the $[\text{Zr}:\text{Ge}]$ ratios are in accord with that of the starting mixture of [3:0.24].

3.2 Structure description

The crystal structures may be regarded as intergrowth structures (Fig. 3), which consist of the NaCl-type $[\text{Zr}_m\text{C}_{m+1}]$ layers (thickness of ~ 0.55 nm for $m = 2$ and ~ 0.83 nm for $m = 3$) separated by the Al_4C_3 -type $[\text{Al}_{4-z}\text{Ge}_z\text{C}_4]$ layers with ~ 0.81 nm thickness ($0 \leq z \leq 0.07$). These two types of layers share the two-dimensional networks of carbon atoms at their boundaries; the C-C distances are 0.3323 nm for $m = 2$ and 0.3319 nm for $m = 3$. These values are close to each other, and also to the C-C distances of the ZrC and Al_4C_3 crystals.

The selected interatomic distances, together with their standard deviations, are given in Tables 5 and 6. The mean interatomic distances in $(\text{ZrC})_2\text{Al}_3[\text{Al}_{0.93}\text{Ge}_{0.07}]\text{C}_3$ and $(\text{ZrC})_3\text{Al}_3[\text{Al}_{0.96}\text{Ge}_{0.04}]\text{C}_3$ compare well with those of ZrC, Al_4C_3 , $(\text{ZrC})_2\text{Al}_3\text{C}_2$, $(\text{ZrC})_3\text{Al}_3\text{C}_2$, $(\text{ZrC})_2\text{Al}_4\text{C}_3$ and $(\text{ZrC})_3\text{Al}_4\text{C}_3$. The Zr sites are octahedrally coordinated by C atoms with the mean distances of 0.237 nm for $m = 2$ and 0.236 nm for $m = 3$, which are comparable to those of the ZrC₈ polyhedra in ZrC (0.235 nm), $(\text{ZrC})_2\text{Al}_3\text{C}_2$ (0.241 nm), $(\text{ZrC})_3\text{Al}_3\text{C}_2$ (0.239 nm), $(\text{ZrC})_2\text{Al}_4\text{C}_3$ (0.237 nm) and $(\text{ZrC})_3\text{Al}_4\text{C}_3$ (0.236 nm).^{1,4,5)} The mean Zr-Al/Ge distances of 0.298 nm for $m = 2$ and 0.300 nm for $m = 3$ are

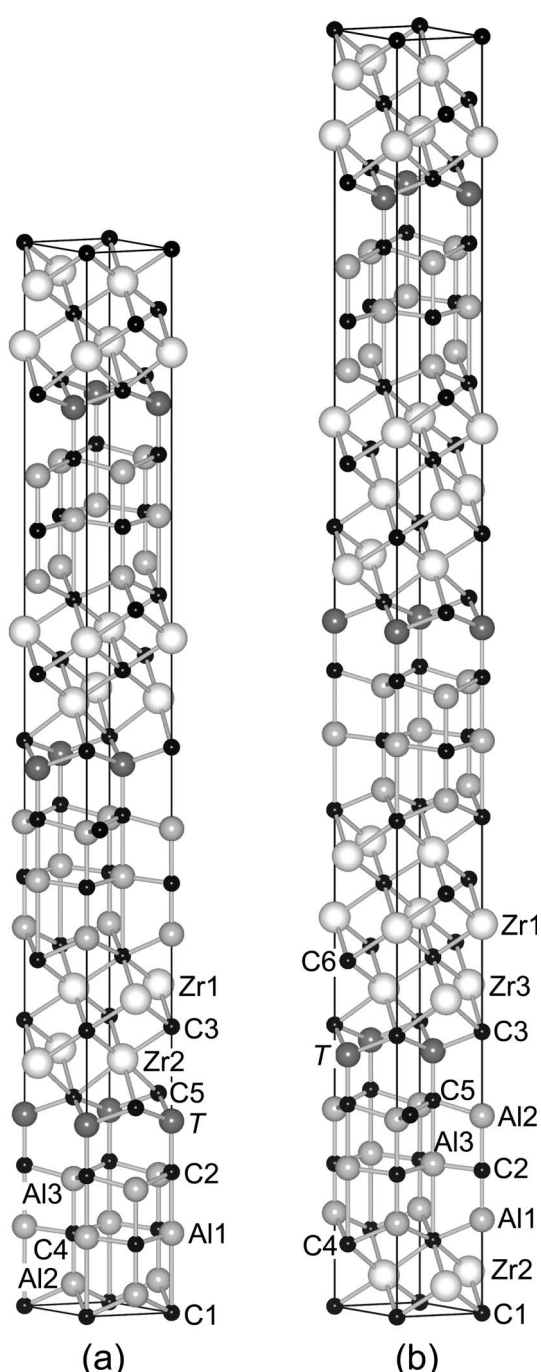


Fig. 3. Crystal structures of $(\text{ZrC})_2\text{Al}_3[\text{Al}_{0.93}\text{Ge}_{0.07}]\text{C}_3$ in (a) and $(\text{ZrC})_3\text{Al}_3[\text{Al}_{0.96}\text{Ge}_{0.04}]\text{C}_3$ in (b). The Ge atoms are exclusively distributed on the T sites for both crystal structures.

Table 5. Interatomic Distances (nm) in $(\text{ZrC})_2\text{Al}_3[\text{Al}_{0.93}\text{Ge}_{0.07}]\text{C}_3^*$

Zr1–C3	0.232(1) × 3
Zr1–C1	0.2336(5) × 3
Zr1–Al2	0.2964(8) × 3
Zr1–Zr2	0.32676(7) × 3
Zr2–C3	0.234(1) × 3
Zr2–C5	0.2468(6) × 3
Zr2–T	0.2993(6) × 3
Al1–C4	0.1927(2) × 3
Al1–C2	0.235(2)
Al1–Al3	0.2717(3) × 3
Al1–Al2	0.2867(8) × 3
Al1–C1	0.306(1)
Al2–C4	0.195(2)
Al2–C1	0.2130(4) × 3
Al3–C2	0.1966(4) × 3
Al3–C4	0.210(2)
Al3–T	0.3065(6) × 3
Al3–C5	0.314(1)
T–C2	0.196(2)
T–C5	0.2058(4) × 3

*All distances shorter than 0.33 nm (metal–metal) and 0.32 nm (metal–carbon) are given.

Table 6. Interatomic Distances (nm) in $(ZrC)_3Al_3[Al_{0.96}Ge_{0.04}]C_3$ ^{*}

Zr1–C6	0.234(2) × 3
Zr1–C1	0.237(2) × 3
Zr1–Zr3	0.3269(3) × 3
Zr1–Zr2	0.3291(3) × 3
Zr2–C1	0.230(2) × 3
Zr2–C4	0.240(1) × 3
Zr2–Al1	0.3000(9) × 3
Zr3–C6	0.232(2) × 3
Zr3–C3	0.243(2) × 3
Zr3–T	0.3002(7) × 3
Al1–C2	0.189(3)
Al1–C4	0.210(1) × 3
Al1–Al3	0.2806(9) × 3
Al2–C5	0.1982(8) × 3
Al2–C2	0.209(3)
Al2–Al3	0.2722(4) × 3
Al2–T	0.3074(8) × 3
Al2–C3	0.322(3)
Al3–C2	0.1922(2) × 3
Al3–C5	0.244(3)
Al3–C4	0.292(3)
T–C5	0.190(3)
T–C3	0.208(1) × 3

*All distances shorter than 0.33 nm (metal–metal) and 0.33 nm (metal–carbon) are given.

comparable to the Zr–Al distances of $(ZrC)_2Al_3C_2$ (0.297 nm), $(ZrC)_3Al_3C_2$ (0.297 nm), $(ZrC)_2Al_4C_3$ (0.299 nm) and $(ZrC)_3Al_4C_3$ (0.302 nm). The Al and T sites are tetrahedrally coordinated with the mean distances of 0.204 nm for both $m = 2$ and $m = 3$. These Al/Ge–C distances are comparable to the Al–C distances of the AlC_4 tetrahedra in Al_4C_3 ranging from

0.194 to 0.218 nm (the mean = 0.206 nm),¹¹⁾ which implies that the $[Al_{4-z}Ge_zC_4]$ layers of both $m = 2$ and $m = 3$ are structurally comparable to the compound Al_4C_3 . Accordingly, these carbide solid solutions form a homologous series with the general formula $(ZrC)_mAl_3[Al_{1-z}Ge_z]C_3$ ($m = 2$ and 3) with $0 \leq z \leq 0.07$.

4. Conclusions

In the Zr–Al–Ge–C system, we have successfully synthesized the two types of new carbide solid solutions $(ZrC)_2Al_3[Al_{1-x}Ge_x]C_3$ ($x = 0.07$) and $(ZrC)_3Al_3[Al_{1-y}Ge_y]C_3$ ($y = 0.04$), the end members of which were, respectively, $(ZrC)_2Al_4C_3$ and $(ZrC)_3Al_4C_3$. The crystal structures were considered to be composed of the NaCl-type $[Zr_mC_{m+1}]$ slabs separated by the Al_4C_3 -type $[Al_{4-z}Ge_zC_4]$ layers, and hence they formed a homologous series with the general formula $(ZrC)_mAl_3[Al_{1-z}Ge_z]C_3$ ($m = 2$ and 3) with $0 \leq z \leq 0.07$.

Acknowledgments Supported by a Grant-in-Aid for Scientific Research (No. 18560654) from the Japan Society for the Promotion of Science, and a grant from the Research Foundation for the Electrotechnology of Cubu.

References

- 1) K. Sugiura, T. Iwata, H. Yoshida, S. Hashimoto and K. Fukuda, *J. Solid State Chem.*, **181**, 2864–2868 (2008).
- 2) K. Fukuda, M. Hisamura, T. Iwata, N. Tera and K. Sato, *J. Solid State Chem.*, **180**, 1809–1815 (2007).
- 3) K. Fukuda, M. Hisamura, Y. Kawamoto and T. Iwata, *J. Mater. Res.*, **22**, 2888–2894 (2007).
- 4) K. Fukuda, S. Mori and S. Hashimoto, *J. Am. Ceram. Soc.*, **88**, 3528–3530 (2005).
- 5) Th. M. Gesing and W. Jeitschko, *J. Solid State Chem.*, **140**, 396–401 (1998).
- 6) F. Izumi and K. Momma, *Solid State Phenom.*, **130**, 15–20 (2007).
- 7) F. Izumi and T. Ikeda, *Mater. Sci. Forum*, **321–324**, 198–203 (2000).
- 8) H. Toraya, *J. Appl. Crystallogr.*, **23**, 485–491 (1990).
- 9) R. A. Young, “The Rietveld Method”, Ed. by R. A. Young, Oxford University Press, Oxford, U. K. (1993) pp. 1–38.
- 10) G. W. Brindley, *Bulletin de la Societe Chimique de France*, D59–63 (1949).
- 11) Th. M. Gesing and W. Jeitschko, *Z. Naturforsch.*, **50b**, 196–200 (1995).